A Monte Carlo study of effects of chain stiffness and chain ends on dilute solution behavior of polymers. I. Gyration-radius expansion factor

Hiromi Yamakawa and Takenao Yoshizaki[a)]
Department of Polymer Chemistry, Kyoto University, Kyoto 606-8501, Japan

(Received 27 September 2002; accepted 18 November 2002)

A Monte Carlo (MC) study is made of the mean-square radius of gyration $\langle S^2 \rangle$ and the gyration-radius expansion factor α_S for the freely rotating chain of bond angle 109° and with the Lennard-Jones (LJ) 6-12 intramolecular potentials between beads in a cutoff version for the number n of bonds in the chain ranging from 10 to 1500 at the reduced temperature ranging from 3.6 to 8.0, which is defined as the absolute temperature multiplied by the Boltzmann constant and divided by the depth of the well of the LJ potential. It is shown that the ratio $\langle S^2 \rangle / n$ approaches asymptotically a constant independent of n for very large n at the value 3.72 ± 0.05 of the reduced temperature, which value is equal to the reduced Θ temperature Θ^* of the MC model system, and that possible effects of chain ends on $\langle S^2 \rangle$ and therefore on α_S are negligibly small. Taking the values of $\langle S^2 \rangle$ at Θ^* as the unperturbed ones, α_S^2 is evaluated from those at various reduced temperatures higher than Θ^*. It is then found that the behavior of α_S^2 may be well explained in the quasi-two-parameter scheme or is in good agreement with that of real experimental data. Further, the binary cluster integral for a bead in the chain is found to be much smaller in magnitude than that for a single isolated bead at reduced temperatures higher than Θ^*, the result being consistent with a previous finding. © *2003 American Institute of Physics.* [DOI: 10.1063/1.1536619]

I. INTRODUCTION

In a series of recent experimental studies of the excluded-volume effects in dilute solutions of oligomers and polymers,[1,2] we have extensively investigated the dependence on molecular weight and solvent condition of expansion factors such as the gyration-radius expansion factor α_S and also the second virial coefficient A_2 for various kinds of flexible polymers. Recall that α_S is defined as the square root of the ratio of the mean-square radius of gyration $\langle S^2 \rangle$ to its unperturbed value $\langle S^2 \rangle_0$ and is a measure of the intramolecular excluded-volume effect, whereas A_2 is concerned with the intermolecular excluded-volume effect. It has then been shown that the behavior of all the expansion factors, including α_S, may be well explained by the quasi-two-parameter (QTP) scheme[1] that all of them are functions only of the intramolecular scaled excluded-volume parameter[1,3,4] $\tilde{z}$ instead of the conventional excluded-volume parameter z in the two-parameter (TP) theory.[5] In the former scheme, the effects of chain stiffness, which become significant as the molecular weight is decreased, are properly taken into account. On the other hand, it has been theoretically shown that an additional parameter named the intermolecular scaled excluded-volume parameter[1] is necessary to introduce in order to explain the behavior of A_2, so that neither the TP nor the QTP scheme is valid for A_2.[1,6] It has been indeed found in consistence with the theory that data points in the plot of the interpenetration function Ψ appearing in A_2 against α_S^3 do not form a single-composite curve because of chain stiffness.[1]

In the course of deriving the above-mentioned conclusions for A_2, possible effects of a chemical difference of the polymer chain ends have been removed[1,7] from observed values of A_2 by the use of the theory[1,6] which takes account of those effects with some assumptions. On the other hand, the effects on the expansion factors may be considered to be negligibly small. For the confirmation of these conclusions, data for a polymer-solvent system without the end effects are therefore desirable to obtain. Unfortunately, however, such a real system is not available. The only possible way to pursue the confirmation is to resort to computer simulation. For this purpose, we start a Monte Carlo (MC) simulation study of both effects of chain stiffness and chain ends on the intra- and intermolecular excluded-volume effects. In this paper as a first step, we investigate $\langle S^2 \rangle$ and verify the validity of the above-mentioned assumption that the effects of chain ends on $\langle S^2 \rangle$ and therefore on α_S are negligibly small.

The model used in the present and forthcoming papers is the freely rotating chain[1,5] with excluded-volume interactions between beads (segments) which are represented by a cutoff version of the Lennard-Jones (LJ) 6-12 potential.[8] The reason for the adoption of the LJ potential is that the model becomes more realistic than does the one only with repulsive interactions. The Θ state may then be realized when repulsive and attractive interactions cancel out each other. This adoption necessarily makes us use an off-lattice model chain to retain precisely the potential form in MC sampling. We also note that the freely rotating chain is adopted in order to take account of the effects of chain stiffness. We have already made a MC study of $\langle S^2 \rangle$ for a polymethylene-like lattice chain[3] only with repulsive interactions, and shown that the MC results for α_S may be well explained in the QTP scheme. However, these results do not necessarily guarantee

a)Electronic mail: yoshizaki@molsci.polym.kyoto-u.ac.jp

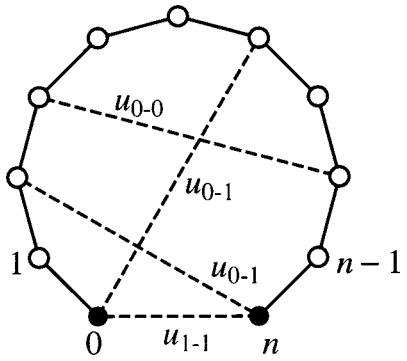

FIG. 1. Three kinds of intramolecular interactions (contacts) between beads.

that those for α_S for the present model with both repulsive and attractive interactions are consistent with the QTP scheme, or with the established experimental results mentioned above. Thus we must also examine whether the present MC results are consistent with the QTP scheme (or the experimental data). This is another purpose of the present paper.

The plan of the present paper is as follows: In Sec. II, we give the definition of the model with excluded-volume interactions between beads. In Sec. III, we give a brief description of the MC simulation algorithm with some basic equations. In Sec. IV, we analyze numerical results so obtained by MC simulation. First, in Sec. IV A, the Θ state for the present model is determined so that the ratio $\langle S^2\rangle/n$ of $\langle S^2\rangle$ to the number n of bonds in the model chain is independent of n in the range of large n. Then, in Sec. IV B, the effects of chain ends are examined by modifying the interactions between the two end beads and between one end and intermediate beads. Finally, in Sec. IV C, α_S is evaluated, and in Sec. IV D, MC results so obtained for it are compared with the QTP theory to examine whether the present MC results compare well with theory and experiment.

II. MODEL

The MC model used in this study is the freely rotating chain[1,5] composed of n bonds, each of length unity, and of $n+1$ beads, whose centers are located at the $n-1$ junctions of two successive bonds and at the two terminal ends. The beads are numbered 0,1,2,...,n from one end to the other, and the ith bond vector $\mathbf{l}_i$ ($|\mathbf{l}_i|=1$) connects the centers of the $(i-1)$th and ith beads with its direction from the $(i-1)$th to the ith bead. All the $n-1$ bond angles θ (not supplements) are fixed at $\theta=109°$, so that the configuration of the entire chain may be specified by the set of $n-2$ internal rotation angles $\{\phi_{n-2}\}=(\phi_2,\phi_3,\ldots,\phi_{n-1})$ apart from its position and orientation in an external Cartesian coordinate system, where ϕ_i is the internal rotation angle around $\mathbf{l}_i$.

In order to examine the effects of chain ends on $\langle S^2\rangle$ and α_S, we consider a rather general case of interactions between beads in which the pair potentials $u_{1\text{-}1}$ between the two end beads, $u_{0\text{-}1}$ between one end and intermediate beads, and $u_{0\text{-}0}$ between intermediate beads are different from each other, as schematically depicted in Fig. 1. For simplicity, we have assumed here that the two end beads are identical to each other in species (compare with Fig. 2 of Ref. 6). Then the total excluded-volume potential energy U of the chain as a function of $\{\phi_{n-2}\}$ may be given by

$$U(\{\phi_{n-2}\})=\sum_{i=1}^{n-5}\sum_{j=i+4}^{n-1}u_{0\text{-}0}(R_{ij})+\sum_{i=4}^{n}u_{0\text{-}1}(R_{0i})+\sum_{i=0}^{n-4}u_{0\text{-}1}(R_{in})+u_{1\text{-}1}(R_{0n}) \tag{1}$$

with R_{ij} the distance between the centers of the ith and jth beads. We must note here that the pairwise decomposability of the potential energy has been assumed, as is usually done in the field.[5] We also note that in Eq. (1) the interactions between the third-neighbor beads along the chain have been neglected, since they seem to make the chain locally take the *cis* conformation to excess. We adopt as the pair potential $u_{\xi\text{-}\eta}(R)$ (of mean force) the cutoff version of the LJ 6-12 potential given by

$$\begin{aligned} u_{\xi\text{-}\eta}(R)&=\infty \quad \text{for } 0\leqslant R<c_{\xi\text{-}\eta}\sigma_{\xi\text{-}\eta}\\ &=u^{\mathrm{LJ}}_{\xi\text{-}\eta}(R) \quad \text{for } c_{\xi\text{-}\eta}\sigma_{\xi\text{-}\eta}\leqslant R<3\sigma_{\xi\text{-}\eta}\\ &=0 \quad \text{for } 3\sigma_{\xi\text{-}\eta}\leqslant R \quad (\xi,\eta=0,1), \end{aligned} \tag{2}$$

where $u^{\mathrm{LJ}}_{\xi\text{-}\eta}(R)$ is the LJ potential[8] given by

$$u^{\mathrm{LJ}}_{\xi\text{-}\eta}(R)=4\epsilon_{\xi\text{-}\eta}\left[\left(\frac{\sigma_{\xi\text{-}\eta}}{R}\right)^{12}-\left(\frac{\sigma_{\xi\text{-}\eta}}{R}\right)^{6}\right] \quad (\xi,\eta=0,1) \tag{3}$$

with $\sigma_{\xi\text{-}\eta}$ and $\epsilon_{\xi\text{-}\eta}$ the collision diameter and the depth of the potential well at the minimum of $u^{\mathrm{LJ}}_{\xi\text{-}\eta}(R)$, respectively. We note that $u^{\mathrm{LJ}}_{\xi\text{-}\eta}(R)$ given by Eqs. (2) is the LJ potential cut off at the upper bound $3\sigma_{\xi\text{-}\eta}$. The lower bound $c_{\xi\text{-}\eta}\sigma_{\xi\text{-}\eta}$ in Eqs. (2) has been introduced for numerical convenience; the factor $c_{\xi\text{-}\eta}$ is properly chosen so that the Boltzmann factor $e^{-u^{\mathrm{LJ}}_{\xi\text{-}\eta}/k_BT}$ may be regarded as numerically vanishing compared to unity, where k_B is the Boltzmann constant and T is the absolute temperature. In practice, in double-precision numerical computation, we put

$$c_{\xi\text{-}\eta}=[2/(1+\sqrt{1+36T^*_{\xi\text{-}\eta}})]^{1/6} \tag{4}$$

so that $e^{-u^{\mathrm{LJ}}_{\xi\text{-}\eta}/k_BT}\leqslant 2\times10^{-16}$ for $0\leqslant R<c_{\xi\text{-}\eta}\sigma_{\xi\text{-}\eta}$, where $T^*_{\xi\text{-}\eta}$ is the reduced temperature defined by $T^*_{\xi\text{-}\eta}=k_BT/\epsilon_{\xi\text{-}\eta}$.

The above-defined MC model has six parameters, i.e., the three $\sigma_{\xi\text{-}\eta}$'s and the three $\epsilon_{\xi\text{-}\eta}$'s (or $T^*_{\xi\text{-}\eta}$'s), in addition to n (and θ). In order to reduce the number of parameters, for convenience, we introduce the Lorentz and Berthelot combining rules, which relate $\sigma_{0\text{-}1}$ to $\sigma_{0\text{-}0}$ and $\sigma_{1\text{-}1}$, and $\epsilon_{0\text{-}1}$ to $\epsilon_{0\text{-}0}$ and $\epsilon_{1\text{-}1}$, respectively, as follows;[8]

$$\sigma_{0\text{-}1}=\tfrac{1}{2}(\sigma_{0\text{-}0}+\sigma_{1\text{-}1}) \quad \text{(Lorentz rule)}, \tag{5}$$

$$\epsilon_{0\text{-}1}=(\epsilon_{0\text{-}0}\epsilon_{1\text{-}1})^{1/2} \quad \text{(Berthelot rule)}. \tag{6}$$

Note that we have $T^*_{0\text{-}1}=(T^*_{0\text{-}0}T^*_{1\text{-}1})^{1/2}$ from Eq. (6). Then the present MC model may be described by the parameters: n, (θ,) $\sigma_{0\text{-}0}$, $\sigma_{1\text{-}1}$, $\epsilon_{0\text{-}0}$ (or $T^*_{0\text{-}0}$), and $\epsilon_{1\text{-}1}$ (or $T^*_{1\text{-}1}$).

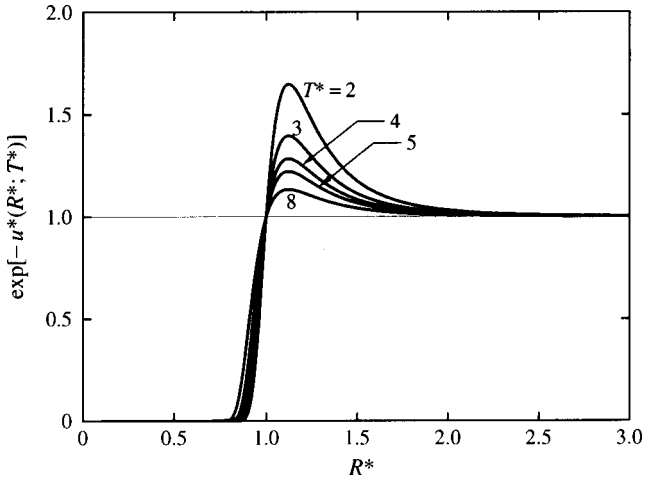

FIG. 2. Plots of $e^{-u^*(R^*;T^*)}$ against the reduced distance R^* for the indicated values of the reduced temperature T^*.

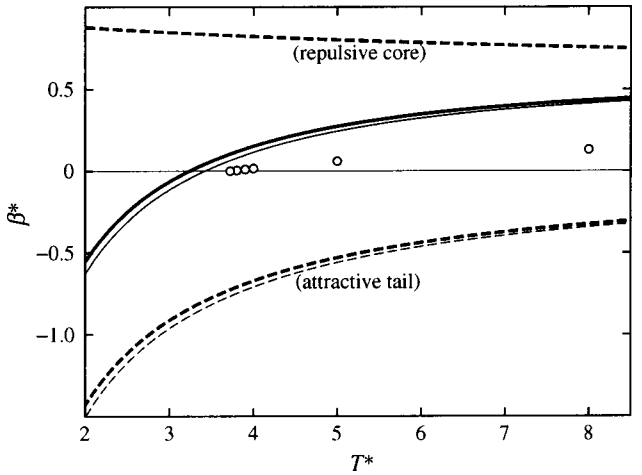

FIG. 3. Plots of β^* against T^*. The heavy solid curve represents the values of β^*, and the upper and lower heavy dashed curves represent the values of the repulsive-core and attractive-tail parts of β^*, respectively. The light solid and dashed curves represent the values of β^* and its attractive-tail part, respectively, calculated with the (original) LJ 6-12 potential. The open circles represent the values of β^* for a bead in the freely rotating chain determined from an analysis of $\langle S^2\rangle$ in the QTP scheme (see the text).

Before proceeding to give a description of the simulation algorithm, it is worthwhile to examine here the behavior of the customary binary-cluster integral[5] for a pair of beads defined by

$$\beta_{\xi\text{-}\eta}=4\pi\int_0^\infty [1-e^{-u_{\xi\text{-}\eta}(R)/k_BT}]R^2\,dR. \tag{7}$$

(Note that $-\beta_{\xi\text{-}\eta}$ is usually called the binary cluster integral.[8]) Let $u^*_{\xi\text{-}\eta}(R)$ be the reduced potential defined by

$$u^*_{\xi\text{-}\eta}(R)=u_{\xi\text{-}\eta}(R)/k_BT=u^*(R^*_{\xi\text{-}\eta};T^*_{\xi\text{-}\eta}), \tag{8}$$

where $R^*_{\xi\text{-}\eta}$ is the reduced distance between beads defined by $R^*_{\xi\text{-}\eta}=R/\sigma_{\xi\text{-}\eta}$. The second of Eqs. (8) indicates that $u_{\xi\text{-}\eta}(R)/k_BT$ is the function u^* of $R^*_{\xi\text{-}\eta}$ and $T^*_{\xi\text{-}\eta}$, the explicit expression for it being omitted.

Values of $e^{-u^*(R^*;T^*)}$ are plotted against the reduced distance R^* in Fig. 2, where the solid curves represent those calculated from the second of Eqs. (8) with Eqs. (2) and (3) for the indicated values of the reduced temperature T^*. (Note that the quantity $e^{-u^*(R^*;T^*)}$ corresponds to the radial distribution function for beads at infinite dilution.[8]) It is seen from Fig. 2 that $e^{-u^*(R^*;T^*)}$ comes very close to its asymptotic value of unity at $R^*=3$ (or $R=3\sigma_{\xi\text{-}\eta}$) at all T^*. Then, let $\beta^*_{\xi\text{-}\eta}$ be the reduced binary-cluster integral defined by

$$\beta^*_{\xi\text{-}\eta}=3\beta_{\xi\text{-}\eta}/4\pi\sigma^3_{\xi\text{-}\eta}=\beta^*(T^*_{\xi\text{-}\eta}). \tag{9}$$

As in Eqs. (8), the second of Eqs. (9) indicates that $3\beta_{\xi\text{-}\eta}/4\pi\sigma^3_{\xi\text{-}\eta}$ is the function β^* of $T^*_{\xi\text{-}\eta}$, the explicit expression for it being also omitted. Figure 3 shows plots of β^* against T^*, where the heavy solid curve represents the values numerically calculated from the second of Eqs. (9) with Eqs. (2), (3), and (7). The upper and lower heavy dashed curves represent the values of the repulsive-core and attractive-tail parts of β^*, respectively, which have been similarly calculated from the second of Eqs. (9) with Eqs. (2), (3), and (7), integrating in Eq. (7) over the ranges from 0 to $\sigma_{\xi\text{-}\eta}$ and from $\sigma_{\xi\text{-}\eta}$ to infinity, respectively. For comparison, the corresponding values calculated with the LJ potential $u^{\mathrm{LJ}}_{\xi\text{-}\eta}$ given by Eq. (3) in place of the cutoff LJ one $u_{\xi\text{-}\eta}$ given by Eq. (2) are also shown in Fig. 3 by the light solid and dashed curves. The values of the repulsive-core part in the original version is numerically identical with those in the cutoff one. Because of the cutoff of the LJ potential at $R=3\sigma_{\xi\text{-}\eta}(R^*=3)$, the values of the attractive-tail part and therefore β^* in the cutoff version are somewhat larger than the corresponding values in the original version. Consequently, the value 3.41_8 of T^* at which β^* vanishes (corresponding to the Boyle temperature) in the original version decreases slightly to 3.23_7 in the cutoff version. In Fig. 3 the open circles represent the values of the binary cluster integral for a bead in the chain evaluated from an analysis of MC results in the QTP scheme, which are given and discussed in Sec. IV D.

III. METHODS

Now we are in a position to give a brief description of the MC simulation algorithm used in this study, which is essentially the same as that used by Stellman and Gans,[9] i.e., the pivot algorithm[10,11] for a sequential generation of chain configurations.

First, we generate an initial configuration $\{\mathbf{l}_n\}=(\mathbf{l}_1,\mathbf{l}_2,\ldots,\mathbf{l}_n)$ by trial and error. A trial set of $n-2$ bond angles $\phi_2,\ \phi_3,\ldots,\phi_{n-1}$ are randomly generated in the interval $[-\pi,\ \pi]$. The first and second bond vectors $\mathbf{l}_1$ and $\mathbf{l}_2$ are fixed so that $\mathbf{l}_1$ is in the direction of the z axis of an external Cartesian coordinate system and $\mathbf{l}_2$ is in the xz plane of the coordinate system with its direction chosen at an obtuse angle with the x axis, i.e., $\mathbf{l}_1=(0,0,1)^T$ and $\mathbf{l}_2=(-\sin\theta,0,-\cos\theta)^T$ with the superscript T indicating the transpose. The succeeding bond vectors $\mathbf{l}_i$ may be given by

$$\mathbf{l}_i=\mathbf{T}(\theta,0)\cdot\mathbf{T}(\theta,\phi_2)\cdot\mathbf{T}(\theta,\phi_3)\cdots\mathbf{T}(\theta,\phi_{i-1})\cdot(0,0,1)^T\quad(i=3,\ldots,n), \tag{10}$$

where $\mathbf{T}(\theta,\phi_{i-1})$ is the orthogonal transformation matrix from the ith to the $(i-1)$th localized Cartesian coordinate system[1] and is given by

$$\mathbf{T}(\theta,\phi)=\begin{pmatrix}\cos\theta\cos\phi & \sin\phi & -\sin\theta\cos\phi\\ \cos\theta\sin\phi & -\cos\phi & -\sin\theta\sin\phi\\ -\sin\theta & 0 & -\cos\theta\end{pmatrix}. \tag{11}$$

The ith localized system associated with $\mathbf{l}_i$ $(i=2,3,...,n)$ is defined as follows. The z_i axis is taken along $\mathbf{l}_i$, the x_i axis is in the plane of $\mathbf{l}_{i-1}$ and $\mathbf{l}_i$ with its direction chosen at an acute angle with $\mathbf{l}_{i-1}$, and the y_i axis completes the right-handed system, so that $\phi_i=0$ in the *trans* conformation. Since the center of the 0th bead is fixed at the origin of the external system, the vector position $\mathbf{r}_i$ of the center of the ith bead $(i=1,2,...,n)$ is given by

$$\mathbf{r}_i=\sum_{j=1}^{i}\mathbf{l}_j. \tag{12}$$

If all the distances between the centers of beads are greater than or equal to $c_{\xi\text{-}\eta}\sigma_{\xi\text{-}\eta}$, the above-given trial configuration is adopted as the initial configuration. If not, this trial is repeated until an initial satisfactory configuration is obtained.

Next the initial configuration $\{\mathbf{l}_n\}$ so obtained is sequentially changed by the pivot algorithm. A trial configuration is generated by rotating the chain with a given present configuration by an angle $\Delta\phi$ randomly chosen in the interval $[-\pi,\pi]$ around a bond randomly chosen from the second through the $(n-1)$th bond. If the pth bond is chosen, the rotation angles ϕ_2', $\phi_3',\ldots,\phi_{n-1}'$ in the trial configuration are given by

$$\phi_i'=\phi_i+\delta_{ip}\Delta\phi \quad (i=2,3,...,n-1). \tag{13}$$

with δ_{ip} the Kronecker delta. In practice, the bond vectors (not the vector positions of the centers of beads) are rotated around $\mathbf{l}_p$ to obtain the set of bond vectors $\{\mathbf{l}_n'\}$ in the trial configuration, whose elements are given by

$$\begin{aligned}\mathbf{l}_i'&=\mathbf{l}_i \quad \text{for } i\leqslant p\\ &=\mathbf{l}_p\mathbf{l}_p\cdot\mathbf{l}_i+(\cos\Delta\phi)(\mathbf{I}-\mathbf{l}_p\mathbf{l}_p)\cdot\mathbf{l}_i+(\sin\Delta\phi)\mathbf{l}_p\times\mathbf{l}_i\\ &\equiv\mathbf{R}(\mathbf{l}_p;\Delta\phi)\cdot\mathbf{l}_i \quad \text{for } i>p,\end{aligned} \tag{14}$$

where $\mathbf{I}$ is the unit matrix and the rotation matrix $\mathbf{R}(\mathbf{l};\Delta\phi)$ is given by

$$\begin{aligned}\mathbf{R}(\mathbf{l};\Delta\phi)=(\cos\Delta\phi)\mathbf{I}&+(1-\cos\Delta\phi)\begin{pmatrix}l_x^2 & l_xl_y & l_xl_z\\ l_yl_x & l_y^2 & l_yl_z\\ l_zl_x & l_zl_y & l_z^2\end{pmatrix}\\ &+\sin\Delta\phi\begin{pmatrix}0 & -l_z & l_y\\ l_z & 0 & -l_x\\ -l_y & l_x & 0\end{pmatrix}\end{aligned} \tag{15}$$

with $\mathbf{l}=(l_x,l_y,l_z)^T$. With this rotation, $\mathbf{l}_i'$ $(i>p)$ is renormalized to $\mathbf{l}_{i(\mathrm{corr})}'$ so that $|\mathbf{l}_{i(\mathrm{corr})}'|=1$, i.e.,

$$\begin{aligned}\mathbf{l}_{i(\mathrm{corr})}'&=\mathbf{l}_i'/(l_{i,x}'^2+l_{i,y}'^2+l_{i,z}'^2)^{1/2}\\ &\simeq[1-\tfrac{1}{2}(l_{i,x}'^2+l_{i,y}'^2+l_{i,z}'^2-1)]\mathbf{l}_i' \quad \text{for } i>p\end{aligned} \tag{16}$$

in order to suppress a roundoff error characteristic of computer work. (Note that $|\mathbf{l}_i'-\mathbf{l}_{i(\mathrm{corr})}'|\ll 1$.) We note that Eq. (16) for the correction in the present case is much simpler than a rather complicated correction procedure proposed by Stellman and Gans,[9] who rotate the vector positions of the centers of beads instead of the bond vectors. The vector positions of the centers of beads in the trial configuration are calculated from Eq. (12) with the corrected $\{\mathbf{l}_n'\}$.

Then, the adoption of the above-given trial configuration as the next one is determined by the METROPOLIS method of importance sampling[12] on the basis of the total potential energies given by Eq. (1) for the trial and present configurations, i.e., the trial configuration is adopted as the next one with the (transition) probability $\tau(\{\phi_{n-2}'\}|\{\phi_{n-2}\})$ defined by

$$\tau(\{\phi_{n-2}'\}|\{\phi_{n-2}\})=\min[1,e^{-[U(\{\phi_{n-2}'\})-U(\{\phi_{n-2}\})]/k_BT}]. \tag{17}$$

If the trial configuration is discarded, the present one is again adopted as the next one. The practical procedure is as follows. If the distance between the centers of beads of a pair is smaller than $c_{\xi\text{-}\eta}\sigma_{\xi\text{-}\eta}$, the trial configuration is discarded and the present one is adopted as the next one. If not, the total potential energy $U(\{\phi_{n-2}'\})$ is calculated from Eq. (1) and the Boltzmann factor in Eq. (17) is evaluated. Then the probability τ is compared with a random number x for $0\leqslant x<1$. If τ is greater than the random number, the trial configuration is adopted as the next one. If not, the present configuration is adopted as the next one. In computing $U(\{\phi_{n-2}'\})$, the "zippering" method[9,13] has been used for a speedy calculation of the double sum in Eq. (1).

By the use of the above-described pivot algorithm, we sample one configuration at every M_{nom} (nominal) pivot steps, and N configurations in total. Then a variable A as a function of $\{\phi_{n-2}\}$ (or $\{\mathbf{l}_n\}$) is calculated for each of the N samples. Finally, the ensemble average $\langle A\rangle$ of A may be evaluated from

$$\langle A\rangle=N^{-1}\sum_{\{\phi_{n-2}\}}A(\{\phi_{n-2}\}), \tag{18}$$

where the sum is taken over the N sample configurations. Note that $N\times M_{\mathrm{nom}}$ pivot steps are required to carry out a MC run.

All the numerical work has been done by the use of a personal computer with an AMD Athlon XP 1500+ CPU. A source program coded in C has been compiled by the GNU C compiler version 2.95.3 with real variables of double precision. For a generation of pseudorandom numbers, we have used the subroutine package MT19937 supplied by Matsumoto and Nishimura[14] instead of the subroutine RAND included in the standard C library. We note that MT19937 is based on the Mersenne Twister algorithm[14] and has an extremely long period of $2^{19937}-1$.

TABLE I. Results of Monte Carlo simulation for $\sigma_{0\text{-}0}=\sigma_{1\text{-}1}=1$ and $T^*_{0\text{-}0}=T^*_{1\text{-}1}$.

n	$10\langle S^2\rangle/n$ (error %)	Acceptance fraction	Number of MC runs
	$T^*_{0\text{-}0}=3.6$		
50	3.58_4 (0.1)	62/100	10
100	3.71_6 (0.2)	103/200	10
200	3.77_3 (0.1)	210/500	10
500	3.74_3 (0.1)	304/1000	5
1000	3.60_8 (0.7)	229/1000	2
	$T^*_{0\text{-}0}=3.7$		
50	3.63_3 (0.1)	63/100	10
100	3.79_0 (0.2)	105/200	10
200	3.89_7 (0.2)	217/500	10
500	3.96_4 (0.1)	327/1000	5
1000	3.95_8 (0.2)	257/1000	5
	$T^*_{0\text{-}0}=3.72$		
10	3.05_8 (0.1)	17/20	10
20	3.33_5 (0.1)	30/40	10
50	3.63_4 (0.2)	63/100	10
100	3.80_4 (0.1)	106/200	10
200	3.91_9 (0.2)	219/500	10
500	4.00_3 (0.1)	331/1000	5
1000	4.01_0 (0.5)	261/1000	5
1500	4.02_7 (0.5)	455/2000	2
	$T^*_{0\text{-}0}=3.8$		
50	3.66_9 (0.1)	63/100	10
100	3.86_0 (0.1)	108/200	10
200	4.00_6 (0.1)	225/500	10
500	4.15_4 (0.2)	346/1000	5
1000	4.21_8 (0.4)	278/1000	2
	$T^*_{0\text{-}0}=3.9$		
50	3.70_5 (0.1)	64/100	10
100	3.92_0 (0.2)	110/200	10
200	4.11_2 (0.1)	232/500	10
500	4.32_7 (0.1)	363/1000	5
1000	4.48_3 (0.1)	300/1000	2
	$T^*_{0\text{-}0}=4.0$		
50	3.74_0 (0.1)	65/100	10
100	3.97_8 (0.1)	112/200	10
200	4.20_1 (0.1)	238/500	10
500	4.48_4 (0.2)	379/1000	5
1000	4.71_0 (0.2)	319/1000	2
	$T^*_{0\text{-}0}=5.0$		
50	3.98_5 (0.1)	70/100	10
100	4.38_9 (0.1)	125/200	10
200	4.82_4 (0.1)	279/500	10
500	5.46_2 (0.1)	480/1000	5
1000	6.01_0 (0.1)	430/1000	2
	$T^*_{0\text{-}0}=8.0$		
50	4.28_7 (0.1)	76/100	10
100	4.86_7 (0.1)	140/200	10
200	5.51_1 (0.2)	324/500	10
500	6.47_2 (0.1)	585/1000	5
1000	7.29_4 (0.1)	542/1000	2

IV. RESULTS AND DISCUSSION

A. Unperturbed state

The mean-square radius of gyration $\langle S^2\rangle$ has been evaluated from Eq. (18), where the squared radius of gyration S^2 for each MC sample has been calculated from

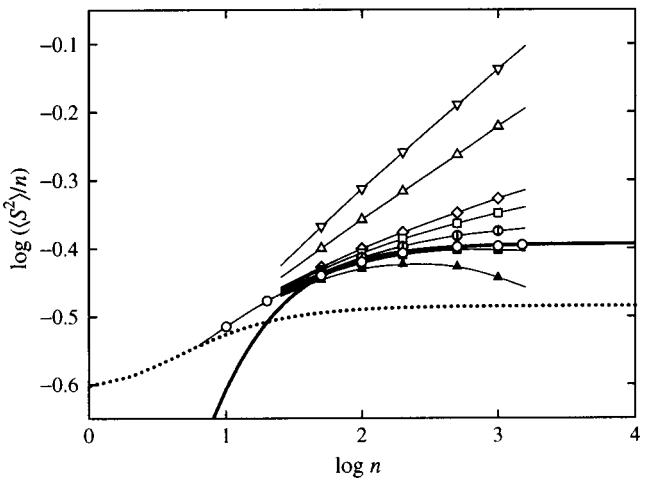

FIG. 4. Double-logarithmic plots of $\langle S^2\rangle/n$ against n for $\sigma_{0\text{-}0}=\sigma_{1\text{-}1}=1$ at $T^*_{0\text{-}0}=T^*_{1\text{-}1}=3.6$ (closed triangle), 3.7 (closed square), 3.72 (open circle), 3.8 (open circle with vertical line segment), 3.9 (open square), 4.0 (diamond), 5.0 (open triangle), and 8.0 (open inverted triangle), the light solid curve connecting smoothly the data points at each T^*. The dotted line segments connect the theoretical values for the ideal freely rotating chain, and the heavy solid curve represents the best-fit KP theoretical values for the data points for $n\geqslant 50$ at $T^*_{0\text{-}0}=T^*_{1\text{-}1}=3.72\,(\Theta^*)$ calculated with $\lambda^{-1}=3.0_1$ and $n_L=1.2_4$.

$$S^2=\frac{1}{n+1}\sum_{i=0}^{n}|\mathbf{r}_i-\mathbf{r}_{\text{c.m.}}|^2 \tag{19}$$

with $\mathbf{r}_{\text{c.m.}}$ the vector position of the center of mass of the sample chain given by

$$\mathbf{r}_{\text{c.m.}}=\frac{1}{n+1}\sum_{i=0}^{n}\mathbf{r}_i\,. \tag{20}$$

All MC runs have been carried out to obtain 10^5 sample configurations.

We have evaluated $\langle S^2\rangle$ for the chains with $n=10-1500$ in the case of $\sigma_{0\text{-}0}=\sigma_{1\text{-}1}=1$ and $T^*_{0\text{-}0}=T^*_{1\text{-}1}$ for several values of $T^*_{0\text{-}0}$ in order to find the unperturbed Θ state in which $\langle S^2\rangle/n$ becomes a constant independent of n for very large n. The results are given in Table I. In Table I, the values of the acceptance fraction, i.e., the mean number of changes in configuration in the M_{nom} pivot steps divided by M_{nom} are given in the third column along with those of the number of MC runs in the fourth column. Specifically, for example, for the chain with $n=50$ at $T^*_{0\text{-}0}=3.6$, 10 independent MC runs have been repeated, in each of which 100×10^5 pivot steps have resulted in 62×10^5 changes in configuration. The values of $\langle S^2\rangle/n$ and its statistical error given in the second column of Table I are those of the mean and the standard deviation, respectively, of the independent MC results.

Figure 4 shows double-logarithmic plots of $\langle S^2\rangle/n$ against n with the MC data given in Table I for $\sigma_{0\text{-}0}=\sigma_{1\text{-}1}=1$ at $T^*_{0\text{-}0}=T^*_{1\text{-}1}=3.6$ (closed triangle), 3.7 (closed square), 3.72 (open circle), 3.8 (open circle with vertical line segment), 3.9 (open square), 4.0 (diamond), 5.0 (open triangle), and 8.0 (open inverted triangle). The light solid curve smoothly connects the data points at each T^*. $\langle S^2\rangle/n$ in-

creases monotonically with increasing n for $T^*_{0\text{-}0} \geqslant 3.8$, while it has a maximum and decreases with increasing n in the range of large n for $T^*_{0\text{-}0} \leqslant 3.6$. The (usual) Θ state[1] may therefore exist in the range of $3.6 < T^*_{0\text{-}0} < 3.8$. At $T^*_{0\text{-}0} = 3.7$ and 3.72, $\langle S^2 \rangle / n$ slightly decreases and increases, respectively, with increasing n for $n \geqslant 500$ (see Table I). On the basis of the present MC results for $\langle S^2 \rangle$, it may be concluded that the reduced Θ temperature $\Theta^* \equiv k_B T / \sigma_{0\text{-}0}$ is 3.72 ± 0.05. Note that this value of Θ^* is appreciably larger than the corresponding value 3.23_7 of T^* for an isolated single bead mentioned in Sec. II. It is then important to note that the (reduced) Θ temperature[1] has a physical meaning completely different from that of the tricritical point[15] determined by Meirovitch and Lim[16] for a self-avoiding walk on a simple cubic lattice with nearest-neighbor attractive cites and by Rubio *et al.*[17] for a MC chain composed of Gaussian bonds and beads with a LJ 6-12 interaction potential. We also note that the Θ temperature has been determined for a MC chain composed of harmonic bonds and beads with a Morse interaction potential.[18]

For comparison, the theoretical values of $\langle S^2 \rangle / n$ for the ideal freely rotating chain without interactions between beads, which have been calculated from

$$\langle S^2 \rangle_0 = \frac{1}{6} \frac{1-\cos\theta}{1+\cos\theta} n + \frac{1}{6} \frac{1+6\cos\theta-\cos^2\theta}{(1+\cos\theta)^2} + \frac{1}{6} \frac{-1-7\cos\theta+7\cos^2\theta+\cos^3\theta}{(1+\cos\theta)^3} \frac{1}{n+1} - \frac{2\cos^2\theta}{(1+\cos\theta)^4} \frac{1-(-\cos\theta)^{n+1}}{(n+1)^2} \tag{21}$$

with $\theta = 109°$, are also shown in Fig. 4, being connected by the dotted line segments. It is seen that the asymptotic value of $\langle S^2 \rangle / n$ in the limit of $n \to \infty$ for the MC data at $T^*_{0\text{-}0} = 3.72 (\Theta^*)$ is appreciably ($\sim$20%) larger than that for the ideal chain, indicating that the unperturbed (Θ) dimension of a polymer chain may be considerably affected by nonbonded interactions, as already pointed out by Bruns[19] on the basis of his MC results for a self-avoiding walk on a simple cubic lattice with nearest-neighbor attractive cites.

For later convenience, we here make an analysis of the present MC data at Θ^* on the basis of the Kratky–Porod (KP) wormlike chain,[1,20] for which (unperturbed) $\langle S^2 \rangle_0$ may be given by[21]

$$\langle S^2 \rangle_0 = \lambda^{-2} f_{S,\mathrm{KP}}(\lambda L) \quad (\mathrm{KP}) \tag{22}$$

with

$$f_{S,\mathrm{KP}}(L) = \frac{L}{6} - \frac{1}{4} + \frac{1}{4L} - \frac{1}{8L^2}(1 - e^{-2L}), \tag{23}$$

where L is the total contour length of the KP chain and λ^{-1} is the stiffness parameter having the dimension of length. In a comparison of theory with MC data, $f_{S,\mathrm{KP}}$ and L may be related to $\langle S^2 \rangle_0 / n$ and n, respectively, as follows:

$$\frac{\langle S^2 \rangle_0}{n} = \frac{\lambda^{-1}}{n_L} \left[\frac{f_{S,\mathrm{KP}}(\lambda L)}{\lambda L} \right], \tag{24}$$

$$\log n = \log(\lambda L) + \log(\lambda^{-1} n_L), \tag{25}$$

TABLE II. Results of Monte Carlo simulation for $\sigma_{0\text{-}0} = \sigma_{1\text{-}1} = 1$ and $T^*_{0\text{-}0} = 3.72 \neq T^*_{1\text{-}1}$.

n	$10\langle S^2 \rangle / n$ (error %)	Acceptance fraction	Number of MC runs
	$T^*_{1\text{-}1} = 2.0$		
10	3.02_3 (0.1)	16/20	10
20	3.29_7 (0.1)	29/40	10
50	3.60_8 (0.1)	62/100	10
100	3.78_1 (0.2)	104/200	10
	$T^*_{1\text{-}1} = 8.0$		
10	3.08_4 (0.1)	17/20	10
20	3.35_9 (0.1)	31/40	10
50	3.65_8 (0.1)	63/100	10
100	3.82_2 (0.1)	107/200	10

where $n_L = n/L$ is the number of bonds per unit contour length and plays the same role as the shift factor[1] M_L in a comparison of theory with experiment.

In Fig. 4 the heavy solid curve represents the best-fit KP theoretical values for the data points for $n \geqslant 50$ at Θ^* calculated from Eqs. (24) and (25) with Eq. (23) with $\lambda^{-1} = 3.0_1$ and $n_L = 1.2_4$. We note that λ^{-1} and n_L so determined here are dimensionless since the bond length has been set equal to unity (or all lengths are measured in units of the bond length). It is seen that the theory reproduces quantitatively the data points for $n \geqslant 50$.

B. Effects of chain ends

Now we examine the effects of chain ends by varying the interaction parameter $\epsilon_{1\text{-}1}(T^*_{1\text{-}1})$ with the others remaining constant as $\sigma_{0\text{-}0} = \sigma_{1\text{-}1} = 1$ and $T^*_{0\text{-}0} = 3.72$. In Table II are given the MC results obtained at $T^*_{1\text{-}1} = 2.0$ and 8.0 in the same manner as that in the case of the results given in Table I. The interaction between the two end beads is strongly attractive and repulsive at $T^*_{1\text{-}1} = 2.0$ and 8.0, respectively, and therefore those between one end and intermediate beads are also attractive and repulsive, respectively. It is found that the difference between the results for a given n at $T^*_{1\text{-}1} = 2.0$ or 8.0 in Table II and at $T^*_{0\text{-}0} = T^*_{1\text{-}1} = 3.72$ in Table I does not exceed 1.2%, the relative difference decreasing with increasing n. Such a small difference cannot be detected experimentally, confirming the validity of the assumption mentioned in Sec. I that the effects of chain ends on $\langle S^2 \rangle$ and therefore on α_S are negligibly small.

C. Gyration-radius expansion factor

In Secs. IV A and IV B, we have shown that the MC results for the freely rotating chain with the LJ 6-12 potential certainly realize the Θ state in the conventional meaning that $\langle S^2 \rangle / n$ there approaches asymptotically a constant independent of n for very large n, and also that the effects of chain ends on $\langle S^2 \rangle / n$ are negligibly small, as usually assumed in an analysis of experimental data. Thus we may analyze the present MC data in the same manner as that in an analysis of experimental data for the excluded-volume effects in real

TABLE III. Values of α_S^2.

	T^*				
n	3.8	3.9	4.0	5.0	8.0
50	1.01_0	1.02_0	1.02_9	1.09_7	1.18_0
100	1.01_5	1.03_0	1.04_6	1.15_4	1.27_9
200	1.02_2	1.04_9	1.07_2	1.23_1	1.40_6
500	1.03_8	1.08_1	1.12_0	1.36_4	1.61_7
1000	1.05_2	1.11_8	1.17_5	1.49_9	1.81_9

polymer solutions, regarding the MC results given in Table I for $\langle S^2\rangle/n$ at $T^*_{0\text{-}0}=\Theta^*(3.72)$ as the unperturbed values $\langle S^2\rangle_0/n$.

In Table III are given the values of the squared gyration-radius expansion factor α_S^2 calculated from

$$\langle S^2\rangle=\langle S^2\rangle_0\alpha_S^2 \tag{26}$$

with the values of $\langle S^2\rangle/n$ given in Table I at $T^*_{0\text{-}0}=3.8$, 3.9, 4.0, 5.0, and 8.0. Figure 5 shows double-logarithmic plots of α_S^2 against n, where the symbols have the same meaning as those in Fig. 4. (See Sec. IV D for the solid curves.) The plots correspond to usual experimental plots of α_S^2 against the degree of polymerization or the molecular weight (see, for example, Fig. 8.5 of Ref. 1). The behavior of the data seems to be similar to that of real experimental data, i.e., the data points at each $T^*_{0\text{-}0}$ follow a curve rising more steeply for larger $T^*_{0\text{-}0}$ with increasing n.

D. Comparison with the QTP theory

We examine whether the behavior of the MC results for α_S^2 determined in Sec. IV C may be well explained in the QTP scheme as in the case of real experimental data for the expansion factors.

Now, according to the QTP scheme or the Yamakawa–Stockmayer–Shimada (YSS) theory,[1,3,4,22] α_S^2 may be given by the Domb–Barrett equation,[23]

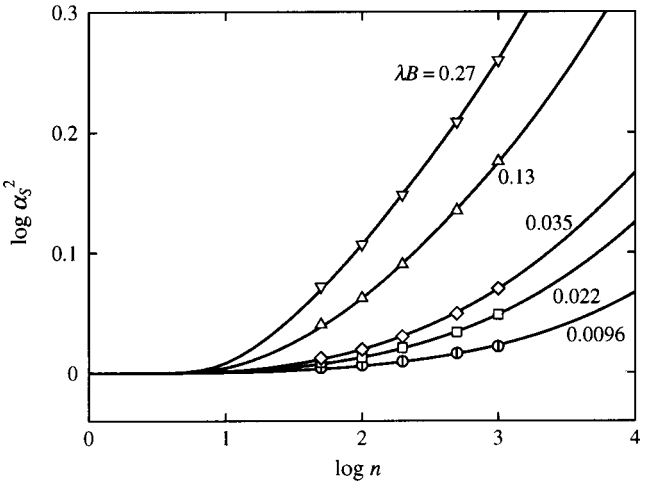

FIG. 5. Double-logarithmic plots of α_S^2 against n. The symbols have the same meaning as those in Fig. 4. The solid curves represent the QTP (or YSS) theory values for the indicated values of λB (see the text).

$$\alpha_S^2=[1+10\tilde{z}+(70\pi/9+10/3)\tilde{z}^2+8\pi^{3/2}\tilde{z}^3]^{2/15}\times[0.933+0.067\exp(-0.85\tilde{z}-1.39\tilde{z}^2)] \tag{27}$$

with the scaled excluded-volume parameter $\tilde{z}$ defined by

$$\tilde{z}=(3/4)K(\lambda L)z \tag{28}$$

in place of the conventional excluded-volume parameter z. The latter is defined by

$$z=(3/2\pi)^{3/2}(\lambda B)(\lambda L)^{1/2} \tag{29}$$

with

$$B=\beta/a^2c_\infty^{3/2}, \tag{30}$$

where β is the binary cluster integral between beads, a is their spacing (in the touched-bead model), and c_∞ is given by

$$c_\infty=\lim_{\lambda L\to\infty}(6\lambda\langle S^2\rangle_0/L)=\frac{4+(\lambda^{-1}\tau_0)^2}{4+(\lambda^{-1}\kappa_0)^2+(\lambda^{-1}\tau_0)^2}. \tag{31}$$

Here, κ_0 and τ_0 are the differential-geometrical curvature and torsion, respectively, of the characteristic helix, i.e., the regular helix that the (unperturbed) helical wormlike (HW) chain[1] takes at the minimum zero of its elastic energy. In the case of the KP chain under consideration, which is a special case of the HW chain with $\kappa_0=0$, the dimensionless factor c_∞ is equal to unity. In Eq. (28), the coefficient $K(L)$ is given by

$$K(L)=\tfrac{4}{3}-2.711L^{-1/2}+\tfrac{7}{6}L^{-1}\quad\text{for } L>6$$
$$=L^{-1/2}\exp(-6.611L^{-1}+0.9198+0.03516L)\quad\text{for } L\leqslant 6. \tag{32}$$

In Fig. 5, the solid curves represent the best-fit QTP (or YSS) theory values calculated from Eq. (27) with Eqs. (25), (28), (29), and (32) with the values of λ^{-1} and n_L determined in Sec. IV A and with the values of $\lambda B=0.0096$, 0.022, 0.035, 0.13, and 0.27 from bottom to top. It is seen that the MC data points at each $T^*_{0\text{-}0}$ closely follow the corresponding theoretical curve, indicating that the present MC data may be well explained in the QTP scheme.

Figure 6 shows double-logarithmic plots of α_S^2 against $\tilde{z}$ with the same MC data as those in Fig. 5, where values of $\tilde{z}$ for the MC data points have been calculated from Eq. (28) with Eqs. (25) and (29) with the above-given values of λB along with the values of λ^{-1} and n_L determined in Sec. IV A. The solid curve represents the QTP (or YSS) theory values calculated from Eq. (27). All the data points follow a single-composite curve and are fitted by the solid curve, as is natural from the results in Fig. 5. This indicates that the present MC model, the freely rotating chain with the LJ 6-12 potential, provides data consistent with experimental ones, so that it may be used to study the effects of chain stiffness and chain ends on other solution properties of polymers.

Finally, we compare the value of the reduced binary-cluster integral β^* for a bead in the freely rotating chain with that for an isolated single bead considered in Sec. II. The values of β^* are evaluated to be 0, 0.0044, 0.010, 0.016, 0.060, and 0.13 at $T^*_{0\text{-}0}(=T^*_{1\text{-}1})=3.72(\Theta^*)$, 3.8, 3.9, 4.0, 5.0, and 8.0, respectively, by dividing β by $4\pi/3$, where β

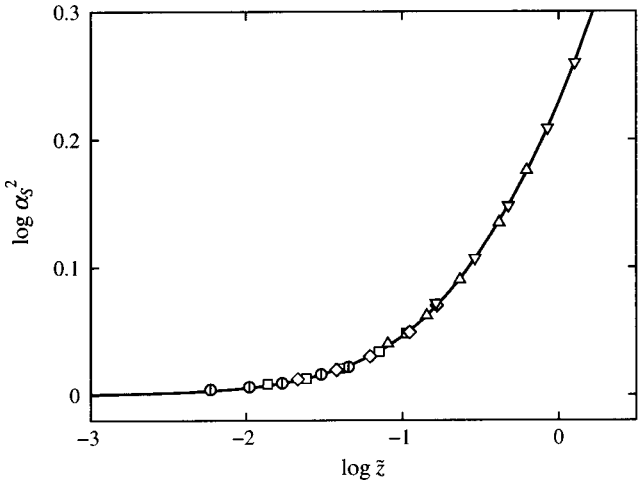

FIG. 6. Double-logarithmic plots of α_S^2 against $\tilde{z}$. The symbols have the same meaning as those in Fig. 4. The solid curve represents the QTP (or YSS) theory values (see the text).

has been calculated from Eq. (30) with the relation $a=n_L^{-1}$ with the above-given values of λB and those of λ^{-1} and n_L determined in Sec. IV A. Naturally, β^* vanishes at Θ^*. These values are shown in Fig. 3 by the open circles. It is interesting to see that the value of β^* in the chain for $T^*_{0\text{-}0} > \Theta^*$ is remarkably smaller in magnitude than that for an isolated single bead at the same $T^*_{0\text{-}0}$. This is consistent with the previous finding that the values of the binary cluster integral per repeat unit (monomer) are one order of magnitude smaller than those for the isolated monomer.[24] The value of β^* in the chain may be considered to come close to that for an isolated single bead as n is decreased to 1. This suggests that the effects of chain ends on A_2 may probably exist even for those polymer chains which have end units almost identical with intermediate ones in chemical structure (without a catalyst fragment at one end).[1,6]

V. CONCLUDING REMARKS

By the present MC simulation of the freely rotating chain with the LJ 6-12 intramolecular potentials between beads in the cutoff version, it has been shown that there certainly exists the reduced Θ temperature Θ^* at which $\langle S^2\rangle/n$ approaches asymptotically a constant independent of the number n of beads in the chain for very large n, and that the effects of chain ends on $\langle S^2\rangle$ and therefore on α_S are negligibly small, as was expected. Taking the values of $\langle S^2\rangle$ at Θ^* as the unperturbed ones, α_S^2 has been evaluated from those at various reduced temperatures higher than Θ^*. It has then been found that the behavior of α_S^2 may be well explained in the QTP scheme or is in good agreement with that of real experimental data, indicating that the MC model may be used to study the effects of chain stiffness and chain ends on other solution properties of polymers. Thus we proceed to make a MC study of A_2 on the basis of the same model in a forthcoming paper, the main purpose of which is to clarify the behavior of A_2 for a fictitious chain without the effects of chain ends, as mentioned in Sec. I.

[1] H. Yamakawa, *Helical Wormlike Chains in Polymer Solutions* (Springer, Berlin, 1997).
[2] F. Abe, Y. Einaga, T. Yoshizaki, and H. Yamakawa, Macromolecules **26**, 1884 (1993), and succeeding papers.
[3] H. Yamakawa and J. Shimada, J. Chem. Phys. **83**, 2607 (1985).
[4] J. Shimada and H. Yamakawa, J. Chem. Phys. **85**, 591 (1986).
[5] H. Yamakawa, *Modern Theory of Polymer Solutions* (Harper & Row, New York, 1971), its electronic edition is available on-line at the URL: http://www.molsci.polym.kyoto-u.ac.jp/archives/redbook.pdf
[6] H. Yamakawa, Macromolecules **25**, 1912 (1992).
[7] Y. Einaga, F. Abe, and H. Yamakawa, Macromolecules **26**, 6243 (1993).
[8] J. P. Hansen and I. R. McDonald, *Theory of Simple Liquids*, 2nd ed. (Academic, London, 1986).
[9] S. D. Stellman and P. J. Gans, Macromolecules **5**, 516 (1972).
[10] M. Lal, Mol. Phys. **17**, 57 (1969).
[11] N. Madras and A. D. Sokal, J. Stat. Phys. **50**, 109 (1988).
[12] N. Metropolis, A. W. Rosenbluth, M. N. Rosenbluth, A. H. Teller, and E. Teller, J. Chem. Phys. **21**, 1087 (1953).
[13] S. D. Stellman, M. Froimowitz, and P. J. Gans, J. Comput. Phys. **7**, 178 (1971).
[14] M. Matsumoto and T. Nishimura, ACM Trans. Model. Comput. Simul. **8**, 3 (1998), see also the URL: http://www.math.keio.ac.jp/matumoto/emt.html
[15] P.-G. de Gennes, *Scaling Concepts in Polymer Physics* (Cornell University Press, Ithaca, 1979).
[16] H. Meitrovitch and H. A. Lim, J. Chem. Phys. **92**, 5144 (1990).
[17] A. M. Rubio, J. J. Freire, J. H. R. Clarke, C. W. Yong, and M. Bishop, J. Chem. Phys. **102**, 2277 (1995).
[18] A. Milchev, W. Paul, and K. Binder, J. Chem. Phys. **99**, 4786 (1993).
[19] W. Bruns, Macromolecules **17**, 2826 (1984).
[20] O. Kratky and G. Porod, Recl. Trav. Chim. Pays-Bas. **68**, 1106 (1949).
[21] H. Benoit and P. Doty, J. Phys. Chem. **57**, 958 (1953).
[22] H. Yamakawa and W. H. Stockmayer, J. Chem. Phys. **57**, 2843 (1972).
[23] C. Domb and A. J. Barrett, Polymer **17**, 179 (1976).
[24] H. Yamakawa, Pure Appl. Chem. **31**, 179 (1972); H. Yamakawa and M. Fujii, J. Chem. Phys. **58**, 1523 (1973).